A method for measuring D^* electromagnetic form factors in e^+e^- annihilation *

Han Guo(郭晗)[1)] Zi-Ping Zhang(张子平)[2)]
University of Science and Technology of China, Hefei 230026, China

Abstract: We describe a method for measuring the electromagnetic form factors of the D^* meson at time-like momentum transfer in e^+e^- annihilation. This is to study the joint angular distribution of the $e^+e^-\to\gamma^*\to D^{*+}D^{*-}$, $D^{*+}\to D^0\pi^+$, and $D^{*-}\to\overline{D}^0\pi^-$ processes. The magnitudes and relative phases of the charge, magnetic and quadrupole form factors can be determined. The method can also be applied to other vector particles.

Keywords: electromagnetic form factor, D^* meson, e^+e^- annihilation, perturbative QCD

PACS: 13.40.Gp, 14.40.Lb, 12.38.Qk **DOI:** 10.1088/1674-1137/41/9/093001

1 Introduction

The electromagnetic interaction is an important probe of the internal structure of hadrons. Figure 1 shows the Feynman diagram for a hadron undergoing an electromagnetic interaction. In the diagram, p is the initial momentum, p' is the final momentum, and $q=p'-p$ is the momentum transfer.

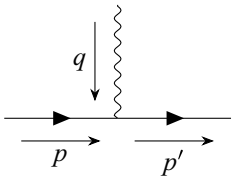

Fig. 1. Feynman diagram for a hadron undergoing electromagnetic interaction.

For a spin 1 particle, assuming parity and time-reversal invariance, the matrix element of the electromagnetic current J^μ can be written as [1–4]

$$\begin{aligned}\langle p'\lambda'|J^\mu|p\lambda\rangle=&-G_1(q^2)\epsilon'^*_{\lambda'}\cdot\epsilon_\lambda(p^\mu+p'^\mu)\\&+G_2(q^2)(\epsilon'^{*\mu}_{\lambda'}\epsilon_\lambda\cdot q-\epsilon^\mu_\lambda\epsilon'^*_{\lambda'}\cdot q)\\&+G_3(q^2)\frac{1}{2M^2}\epsilon_\lambda\cdot q\epsilon'^*_{\lambda'}\cdot q(p^\mu+p'^\mu).\end{aligned}\quad(1)$$

ϵ_λ ($\lambda=0,\pm1$) are polarization vectors of the initial state and $\epsilon'_{\lambda'}$ ($\lambda'=0,\pm1$) the final state. M is the particle mass. The scalar functions G_1, G_2 and G_3 are related to the charge form factor $G_{\rm C}$, magnetic form factor $G_{\rm M}$ and quadrupole form factor $G_{\rm Q}$ [3, 4]:

$$G_{\rm C}=G_1+\frac{2}{3}\eta G_{\rm Q},\quad(2)$$

$$G_{\rm M}=G_2,\quad(3)$$

$$G_{\rm Q}=G_1-G_2+(1+\eta)G_3,\quad(4)$$

where $\eta=-q^2/4M^2$. The charge, magnetic and quadrupole form factors correspond to spatial distributions of charge, magnetic moment and quadrupole moment, respectively, by Fourier transform. Therefore, measuring the electromagnetic form factors gives information on the hadron structure. Perturbative quantum chromodynamics (QCD) predicted the form factors to have the ratios $G_{\rm C}:G_{\rm M}:G_{\rm Q}=(1-\frac{2}{3}\eta):2:-1$ at large space-like or time-like momentum transfer [4].

In this paper we propose a method for measuring the electromagnetic form factors of the D^* meson at time-like momentum transfer. This is to study the $e^+e^-\to\gamma^*\to D^{*+}D^{*-}$ process. The D^* electromagnetic current matrix element is transformed from Equation (1), which is for space-like momentum transfer, to be

$$\begin{aligned}\langle k'\lambda'|J^\mu|k\lambda\rangle=&-G_1(q^2)\epsilon'^*_{\lambda'}\cdot\epsilon^*_\lambda(k'^\mu-k^\mu)\\&+G_2(q^2)(\epsilon'^{*\mu}_{\lambda'}\epsilon^*_\lambda\cdot q-\epsilon^{*\mu}_\lambda\epsilon'^*_{\lambda'}\cdot q)\\&+G_3(q^2)\frac{1}{2M^2}\epsilon^*_\lambda\cdot q\epsilon'^*_{\lambda'}\cdot q(k'^\mu-k^\mu).\end{aligned}\quad(5)$$

k and k' are the momenta of D^{*+} and D^{*-}, respectively. $q=k+k'$ in this case. The differential cross section can then be calculated to be

$$\frac{{\rm d}\sigma}{{\rm d}\Omega}=K(C_1+C_2\cos^2\theta),\quad(6)$$

Received 28 April 2017
∗ Supported by National Natural Science Foundation of China (11675166)
1) E-mail: guohan@mail.ustc.edu.cn
2) E-mail: zpz@ustc.edu.cn

where Ω is the solid angle of D^{*+} in the center-of-mass frame (CM) and θ is the polar angle.

$$K=\frac{\alpha_{\rm em}^2}{8E_{\rm CM}^2}\left(1-\frac{M^2}{E^2}\right)^{\frac{3}{2}}, \tag{7}$$

in which $\alpha_{\rm em}$ is the fine-structure constant, $E_{\rm CM}$ is the total energy in CM, $E=E_{\rm CM}/2$ is the energy of D^* in CM, and M is the D^* mass.

$$C_1=3|G_{\rm C}|^2-2\eta|G_{\rm M}|^2+\frac{8}{3}\eta^2|G_{\rm Q}|^2, \tag{8}$$

$$C_2=-3|G_{\rm C}|^2-2\eta|G_{\rm M}|^2-\frac{8}{3}\eta^2|G_{\rm Q}|^2, \tag{9}$$

with $\eta=-q^2/4M^2=-E^2/M^2$. The total cross section is

$$\sigma=4\pi K(C_1+\frac{C_2}{3}). \tag{10}$$

C_1 and C_2 can be obtained by measuring the angular distribution $\sim 1+C_2/C_1\cos^2\theta$ and the total cross section $\sim C_1+C_2/3$. Then from

$$C_1+C_2=-4\eta|G_{\rm M}|^2, \tag{11}$$

$$C_1-C_2=6|G_{\rm C}|^2+\frac{16}{3}\eta^2|G_{\rm Q}|^2, \tag{12}$$

we can obtain $|G_{\rm M}|$ and a linear combination of $|G_{\rm C}|^2$ and $|G_{\rm Q}|^2$. However, we cannot determine $|G_{\rm C}|$ and $|G_{\rm Q}|$ individually. Moreover, the phases of the form factors are absent from the differential cross section formula. They are contained in the spin states of the particles and therefore show in the angular distributions of subsequent decays. In this spirit we shall study also the angular distributions of the $D^{*+}\to D^0\pi^+$ and $D^{*-}\to\overline{D}^0\pi^-$ decays.

2 Method

2.1 Joint differential cross section

For the $e^+e^-\to\gamma^*\to D^{*+}D^{*-}$, $D^{*+}\to D^0\pi^+$, $D^{*-}\to\overline{D}^0\pi^-$ process, we calculate its joint differential cross section to be

$$\frac{{\rm d}\sigma}{{\rm d}\cos\theta{\rm d}\alpha{\rm d}\cos\beta{\rm d}\alpha'{\rm d}\cos\beta'}=\frac{K}{8\pi}f(\theta,\alpha,\beta,\alpha',\beta'), \tag{13}$$

where the angles θ, α, β, α' and β' are defined in the reference frames as shown in Fig. 2.

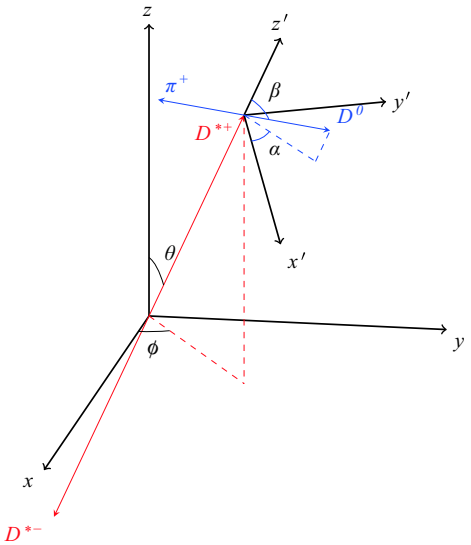

Fig. 2. (color online) Reference frames for describing the D^* pair production and subsequent decays. In the center-of-mass frame (CM) xyz D^{*+} has polar angle θ and azimuthal angle ϕ. The z' axis of the D^{*+} rest frame $x'y'z'$ is along the D^{*+} direction in CM and the x' axis has the same azimuthal angle ϕ in CM as D^{*+}. In $x'y'z'$ D^0 has polar angle β and azimuthal angle α. The D^{*-} rest frame can be defined in the same way. In that frame $\overline{D}^0$ has polar angle β' and azimuthal angle α'.

$$\begin{aligned}f(\theta,\alpha,\beta,\alpha',\beta')=&(R_{\rm C}^2A(\alpha,\beta,\alpha',\beta')+4R_{\rm Q}^2B(\alpha,\beta,\alpha',\beta')+R_{\rm C}R_{\rm Q}\cos(\delta_{\rm C}-\delta_{\rm Q})C(\alpha,\beta,\alpha',\beta'))\sin^2\theta\\&+R_{\rm M}^2(D(\alpha,\beta,\alpha',\beta')\cos^2\theta+E(\alpha,\beta,\alpha',\beta'))+2(R_{\rm C}R_{\rm M}\cos(\delta_{\rm C}-\delta_{\rm M})F(\alpha,\beta,\alpha',\beta')\\&+2R_{\rm M}R_{\rm Q}\cos(\delta_{\rm M}-\delta_{\rm Q})G(\alpha,\beta,\alpha',\beta'))\cos\theta\sin\theta,\end{aligned} \tag{14}$$

in which

$$A(\alpha,\beta,\alpha',\beta')=(\cos(\alpha+\alpha')\sin\beta\sin\beta'+\cos\beta\cos\beta')^2, \tag{15}$$

$$B(\alpha,\beta,\alpha',\beta')=(\cos(\alpha+\alpha')\sin\beta\sin\beta'-2\cos\beta\cos\beta')^2, \tag{16}$$

$$C(\alpha,\beta,\alpha',\beta')=(2\cos(\alpha+\alpha')\sin\beta\sin\beta'-\cos\beta\cos\beta')^2-9\cos^2\beta\cos^2\beta', \tag{17}$$

$$D(\alpha,\beta,\alpha',\beta')=(\cos\alpha\sin\beta\cos\beta'-\cos\alpha'\cos\beta\sin\beta')^2, \tag{18}$$

$$E(\alpha,\beta,\alpha',\beta')=(\sin\alpha\sin\beta\cos\beta'+\sin\alpha'\cos\beta\sin\beta')^2, \tag{19}$$

$$F(\alpha,\beta,\alpha',\beta')=(\cos(\alpha+\alpha')\sin\beta\sin\beta'+\cos\beta\cos\beta')(\cos\alpha\sin\beta\cos\beta'-\cos\alpha'\cos\beta\sin\beta'), \tag{20}$$

$$G(\alpha,\beta,\alpha',\beta')=(\cos(\alpha+\alpha')\sin\beta\sin\beta'-2\cos\beta\cos\beta')(\cos\alpha\sin\beta\cos\beta'-\cos\alpha'\cos\beta\sin\beta'). \tag{21}$$

$$R_{\rm C}=3|G_{\rm C}|, \tag{22}$$
$$R_{\rm M}=3r|G_{\rm M}|, \tag{23}$$
$$R_{\rm Q}=r^2|G_{\rm Q}|, \tag{24}$$

where $r=E/M$. $\delta_{\rm C}$, $\delta_{\rm M}$ and $\delta_{\rm Q}$ are phase angles of the corresponding form factors. Parity conservation and time-reversal invariance are implied for the formula as in Equation (1).

2.2 Angular distribution

Only relative values of the phase angles are meaningful. Thus for convenience we define $\delta_M=0$. Factoring out $R_{\rm M}^2$ and defining

$$r_{\rm C}=\frac{R_{\rm C}}{R_{\rm M}}=\frac{1}{r}\frac{|G_{\rm C}|}{|G_{\rm M}|}, \tag{25}$$
$$r_{\rm Q}=\frac{R_{\rm Q}}{R_{\rm M}}=\frac{r}{3}\frac{|G_{\rm Q}|}{|G_{\rm M}|}, \tag{26}$$

Equation (14) reduces to

$$\begin{aligned}f(\theta,\alpha,\beta,\alpha',\beta')=&(r_{\rm C}^2A(\alpha,\beta,\alpha',\beta')+4r_{\rm Q}^2B(\alpha,\beta,\alpha',\beta')\\&+r_{\rm C}r_{\rm Q}\cos(\delta_{\rm C}-\delta_{\rm Q})C(\alpha,\beta,\alpha',\beta'))\sin^2\theta\\&+D(\alpha,\beta,\alpha',\beta')\cos^2\theta+E(\alpha,\beta,\alpha',\beta')\\&+2(r_{\rm C}\cos\delta_{\rm C}F(\alpha,\beta,\alpha',\beta')\\&+2r_{\rm Q}\cos\delta_{\rm Q}G(\alpha,\beta,\alpha',\beta'))\cos\theta\sin\theta. \end{aligned}\tag{27}$$

We can obtain $r_{\rm C}$, $r_{\rm Q}$, $\delta_{\rm C}$ and $\delta_{\rm Q}$ by fitting $f(\theta,\alpha,\beta,\alpha',\beta')$ to the angular distribution. It is best to have an estimation of the parameter values before fitting. For this we use the following procedure.

2.3 Parameter extraction

We show the procedure with a Monte Carlo (MC) sample distributed according to $f(\theta,\alpha,\beta,\alpha',\beta')$ with the parameter values

$$\begin{aligned}r_{\rm C}&=0.3,\\ r_{\rm Q}&=0.1,\\ \delta_{\rm C}&=60,\\ \delta_{\rm Q}&=45,\end{aligned}$$

where $\delta_{\rm C}$ and $\delta_{\rm Q}$ are in degrees.

We use 0) to represent the entire sample and classify the events into four sub-samples:

1) $F(\alpha,\beta,\alpha',\beta')>0$ and $G(\alpha,\beta,\alpha',\beta')>0$,
2) $F(\alpha,\beta,\alpha',\beta')<0$ and $G(\alpha,\beta,\alpha',\beta')<0$,
3) $F(\alpha,\beta,\alpha',\beta')>0$ and $G(\alpha,\beta,\alpha',\beta')<0$,
4) $F(\alpha,\beta,\alpha',\beta')<0$ and $G(\alpha,\beta,\alpha',\beta')>0$.

The cosθ distributions of 0), 1), 2), 3) and 4) are shown in Fig. 3 and Fig. 4.

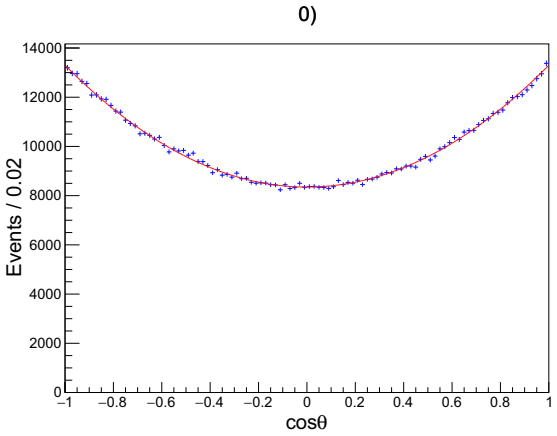

Fig. 3. (color online) The cosθ distribution of the entire Monte Carlo sample. The curve is the fit with $f_0(\theta)$.

The corresponding distribution function for i) ($i=0,1,2,3,4$) is obtained by integrating $f(\theta,\alpha,\beta,\alpha',\beta')$ over α, cosβ, α' and cosβ' under the conditions of i):

$$\begin{aligned}f_i(\theta)=&\left(r_{\rm C}^2A_i+4r_{\rm Q}^2B_i+r_{\rm C}r_{\rm Q}\cos(\delta_{\rm C}-\delta_{\rm Q})C_i\right)\sin^2\theta\\&+D_i\cos^2\theta+E_i\\&+2(r_{\rm C}\cos\delta_{\rm C}F_i+2r_{\rm Q}\cos\delta_{\rm Q}G_i)\cos\theta\sin\theta\end{aligned}\tag{28}$$

where

$$A_0=\frac{1}{2}B_0=\frac{3}{2}D_0=\frac{3}{2}E_0=\frac{16}{3}\pi^2, \tag{29}$$
$$C_0=F_0=G_0=0, \tag{30}$$
$$A_1=A_2=15.09, \tag{31}$$
$$B_1=B_2=22.12, \tag{32}$$
$$C_1=C_2=-C_3=-C_4=56.31, \tag{33}$$
$$D_1=D_2=E_1=E_2=8.71, \tag{34}$$
$$F_1=-F_2=6.82, \tag{35}$$
$$G_1=-G_2=10.61, \tag{36}$$
$$A_3=A_4=11.23, \tag{37}$$
$$B_3=B_4=30.52, \tag{38}$$
$$D_3=D_4=E_3=E_4=8.84, \tag{39}$$
$$F_3=-F_4=6.34, \tag{40}$$
$$G_3=-G_4=-12.26 \tag{41}$$

are the integral values for $A(\alpha,\beta,\alpha',\beta')$, $B(\alpha,\beta,\alpha',\beta')$, ... $G(\alpha,\beta,\alpha',\beta')$. The integral values are calculated numerically except for 0).

Define

$$a_0=A_0(r_{\rm C}^2+8r_{\rm Q}^2), \tag{42}$$
$$a=r_{\rm C}^2A_1+4r_{\rm Q}^2B_1+r_{\rm C}r_{\rm Q}\cos(\delta_{\rm C}-\delta_{\rm Q})C_1, \tag{43}$$
$$b=r_{\rm C}\cos\delta_{\rm C}F_1+2r_{\rm Q}\cos\delta_{\rm Q}G_1, \tag{44}$$
$$a'=r_{\rm C}^2A_3+4r_{\rm Q}^2B_3+r_{\rm C}r_{\rm Q}\cos(\delta_{\rm C}-\delta_{\rm Q})C_3, \tag{45}$$
$$b'=r_{\rm C}\cos\delta_{\rm C}F_3+2r_{\rm Q}\cos\delta_{\rm Q}G_3. \tag{46}$$

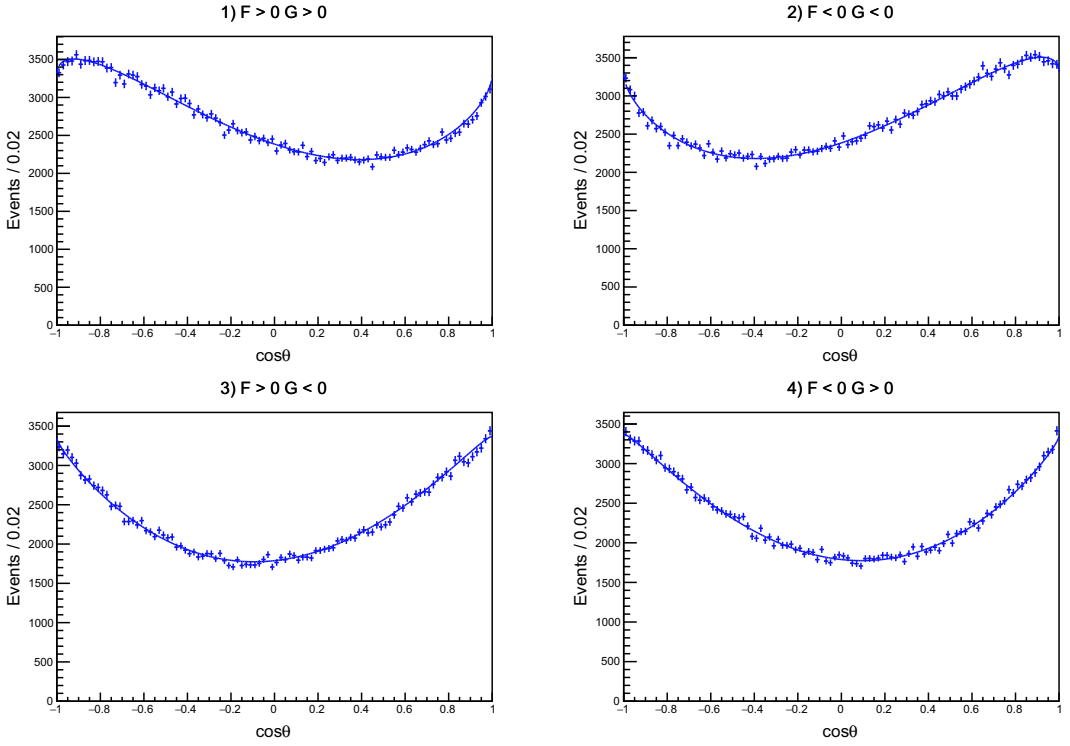

Fig. 4. (color online) The cosθ distributions of the four sub-samples. The curves are the corresponding distribution functions $f_i(\theta)$ (i=1,2,3,4).

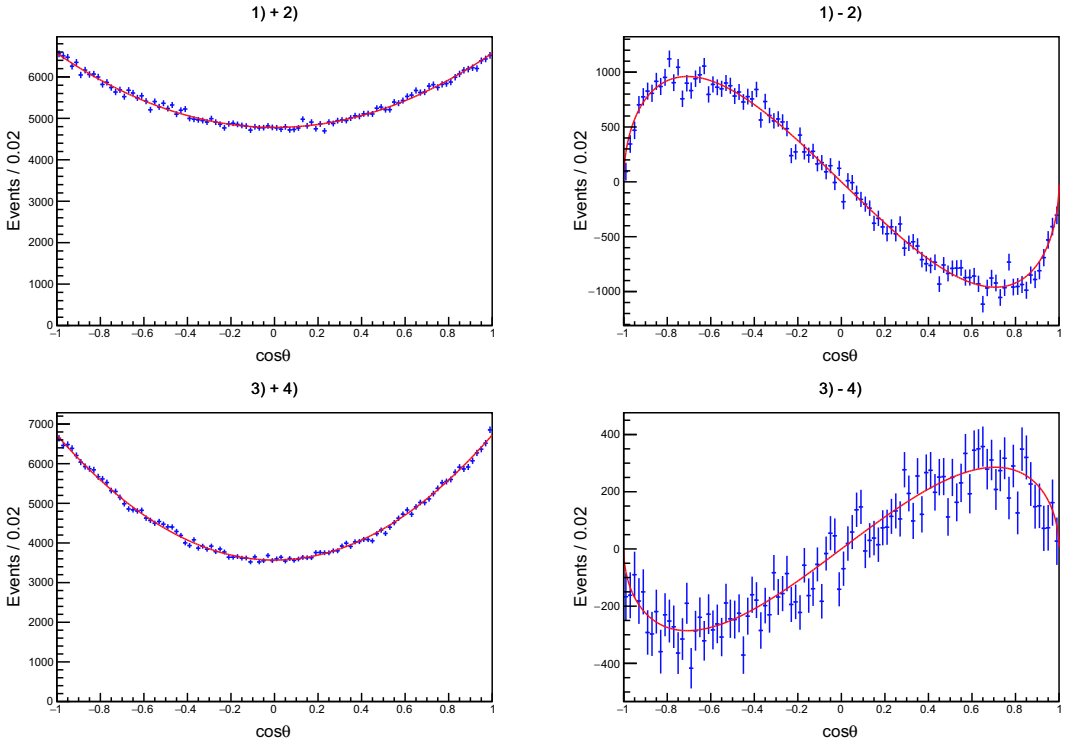

Fig. 5. (color online) The addition and subtraction of the distributions of 1) and 2), and 3) and 4). The curves are fits to them with the corresponding functions.

$f_i(\theta)$ can then be written as

$$f_0(\theta)=D_0+a_0+(D_0-a_0)\cos^2\theta, \quad (47)$$
$$f_1(\theta)=D_1+a+(D_1-a)\cos^2\theta+2b\cos\theta\sin\theta, \quad (48)$$
$$f_2(\theta)=D_1+a+(D_1-a)\cos^2\theta-2b\cos\theta\sin\theta, \quad (49)$$
$$f_3(\theta)=D_3+a'+(D_3-a')\cos^2\theta+2b'\cos\theta\sin\theta, \quad (50)$$
$$f_4(\theta)=D_3+a'+(D_3-a')\cos^2\theta-2b'\cos\theta\sin\theta \quad (51)$$

with the normalizing factors

$$S_0=\frac{4}{3}(2D_0+a_0), \quad (52)$$
$$S_1=S_2=\frac{4}{3}(2D_1+a), \quad (53)$$
$$S_3=S_4=\frac{4}{3}(2D_3+a'). \quad (54)$$

a_0 can be obtained by fitting $f_0(\theta)/S_0$ to the $\cos\theta$ distribution of 0). The fit is shown in Fig. 3. a, b, a', b' can be obtained by fitting

$$\frac{f_1(\theta)}{S_1}+\frac{f_2(\theta)}{S_2}=\frac{2(D_1+a+(D_1-a)\cos^2\theta)}{S_1}, \quad (55)$$
$$\frac{f_1(\theta)}{S_1}-\frac{f_2(\theta)}{S_2}=\frac{4b\cos\theta\sin\theta}{S_1}, \quad (56)$$
$$\frac{f_3(\theta)}{S_3}+\frac{f_4(\theta)}{S_4}=\frac{2(D_3+a'+(D_3-a')\cos^2\theta)}{S_3}, \quad (57)$$
$$\frac{f_3(\theta)}{S_3}-\frac{f_4(\theta)}{S_4}=\frac{4b'\cos\theta\sin\theta}{S_3} \quad (58)$$

to the addition and subtraction of the $\cos\theta$ distributions of 1) and 2), and 3) and 4), respectively. The fits are shown in Fig. 5.

Equation (42) can be obtained by adding Equations (43) and (45) using $A_0=A_1+A_2+A_3+A_4=2(A_1+A_3)$ and similar relations. Thus Equation (45) is duplicate. $r_{\rm Q}^2$ can be expressed in terms of $r_{\rm C}^2$ by Equation (42):

$$r_{\rm Q}^2=\frac{1}{8}(\frac{a_0}{A_0}-r_{\rm C}^2). \quad (59)$$

We define

$$X=r_{\rm C}\cos\delta_{\rm C}, \quad (60)$$
$$Y=r_{\rm Q}\cos\delta_{\rm Q}. \quad (61)$$

Equations (44) and (46) form an equation group:

$$F_1X+2G_1Y=b, \quad (62)$$
$$F_3X+2G_3Y=b'. \quad (63)$$

X and Y can then be solved. With the expression

$$\begin{aligned} r_{\rm C}r_{\rm Q}\cos(\delta_{\rm C}-\delta_{\rm Q})&=r_{\rm C}r_{\rm Q}(\cos\delta_{\rm C}\cos\delta_{\rm Q}+\sin\delta_{\rm C}\sin\delta_{\rm Q})\\ &=XY+r_{\rm C}r_{\rm Q}(\pm\sqrt{1-\cos^2\delta_{\rm C}})\\ &\quad\times(\pm\sqrt{1-\cos^2\delta_{\rm Q}})\\ &=XY\pm\sqrt{(r_{\rm C}^2-X^2)(r_{\rm Q}^2-Y^2)}, \end{aligned} \quad (64)$$

Equation (43) can be transformed:

$$A_1r_{\rm C}^2+4B_1r_{\rm Q}^2+C_1\left(XY\pm\sqrt{(r_{\rm C}^2-X^2)(r_{\rm Q}^2-Y^2)}\right)=a, \quad (65)$$

$$C_1\left(XY\pm\sqrt{(r_{\rm C}^2-X^2)(r_{\rm Q}^2-Y^2)}\right)=a-A_1r_{\rm C}^2-4B_1r_{\rm Q}^2, \quad (66)$$

$$XY\pm\sqrt{(r_{\rm C}^2-X^2)(r_{\rm Q}^2-Y^2)}=\frac{a-A_1r_{\rm C}^2-4B_1r_{\rm Q}^2}{C_1}, \quad (67)$$

$$\pm\sqrt{(r_{\rm C}^2-X^2)(r_{\rm Q}^2-Y^2)}=\frac{a-A_1r_{\rm C}^2-4B_1r_{\rm Q}^2}{C_1}-XY, \quad (68)$$

$$(r_{\rm C}^2-X^2)(r_{\rm Q}^2-Y^2)=\left(\frac{a-A_1r_{\rm C}^2-4B_1r_{\rm Q}^2}{C_1}-XY\right)^2, \quad (69)$$

$$(r_{\rm C}^2-X^2)(r_{\rm Q}^2-Y^2)-\left(\frac{a-A_1r_{\rm C}^2-4B_1r_{\rm Q}^2}{C_1}-XY\right)^2=0. \quad (70)$$

Putting in Equation (59), and defining $x=r_{\rm C}^2$, the equation becomes

$$\begin{aligned} &(x-X^2)\left(\frac{1}{8}\left(\frac{a_0}{A_0}-x\right)-Y^2\right)\\ &-\left(\frac{a-A_1x-\frac{1}{2}B_1\left(\frac{a_0}{A_0}-x\right)}{C_1}-XY\right)^2=0. \end{aligned} \quad (71)$$

The left-hand-side of the equation is a quadratic function of x. We call this function $g(x)$. Figure 6 shows the original $g(x)$ with the default setting values of $r_{\rm C}$, $r_{\rm Q}$, $\delta_{\rm C}$ and $\delta_{\rm Q}$, and $g(x)$ with a_0, a, X and Y we obtained.

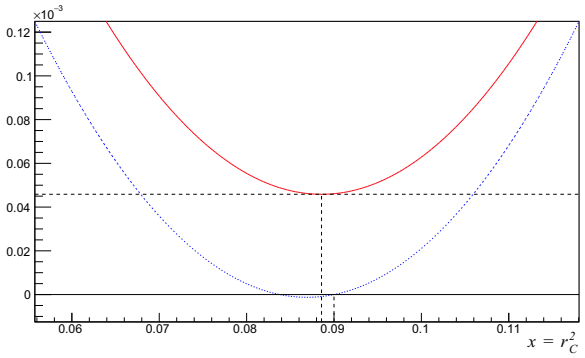

Fig. 6. (color online) The dotted curve is the original $g(x)$ with the default setting values of the parameters. The solid curve is $g(x)$ with the quantities we obtained. The vertical dashed line below the original $g(x)$ is at the default setting value of $r_{\rm C}^2$. The vertical dashed line below the $g(x)$ with the obtained quantities indicates its lowest point.

The $g(x)$ with the obtained quantities is slightly shifted from the original $g(x)$. Although it does not intersect with the x axis, we can take the point closest to the x axis as the approximate solution for x. Hence we

obtain $r_{\rm C}=\sqrt{x}$. From Equations (59), (60) and (61) we also obtain $r_{\rm Q}$, $\delta_{\rm C}$ and $\delta_{\rm Q}$. The results are

$$r_{\rm C}=0.298,$$
$$r_{\rm Q}=0.101,$$
$$\delta_{\rm C}=59.1,$$
$$\delta_{\rm Q}=46.1.$$

They are close to the default setting values of $r_{\rm C}=0.3$, $r_{\rm Q}=0.1$, $\delta_{\rm C}=60$ and $\delta_{\rm Q}=45$. The uncertainties of the parameters are to be given by a combined fit described as follows.

2.4 Combined fit

We combine the distributions of 1), 2), 3) and 4) as shown in Fig. 4 into one, and fit it with the corresponding functions $f_i(\theta)$ combined. In the fit, we take the previous results as the initial values for the parameters. The fit is shown in Fig. 7.

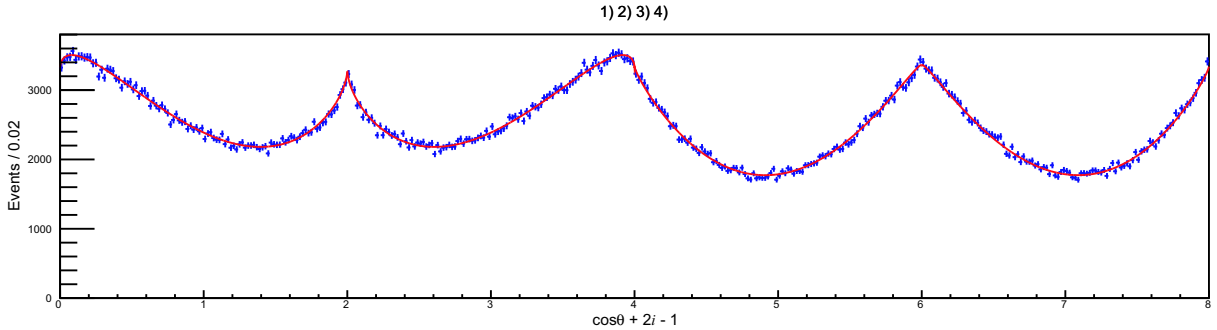

Fig. 7. (color online) The combined distribution of 1), 2), 3) and 4). The curve is the fit with $f_i(\theta)$ combined.

The results are

$$N=999627.1\pm999.8,$$
$$r_{\rm C}=0.301\pm0.045,$$
$$r_{\rm Q}=0.100\pm0.016,$$
$$\delta_{\rm C}=59.5\pm4.9,$$
$$\delta_{\rm Q}=45.3\pm8.8,$$

where N is the total number of events.

2.5 Full fit

Now we can fit $f(\theta,\alpha,\beta,\alpha',\beta')$ to the 5 dimensional angular distribution. We use the extended maximum likelihood fit. The combined fit results are taken as the initial values and uncertainties. The full fit results are

$$N=1000001.2\pm1000.0,$$
$$r_{\rm C}=0.299\pm0.001,$$
$$r_{\rm Q}=0.101\pm0.001,$$
$$\delta_{\rm C}=59.2\pm0.4,$$
$$\delta_{\rm Q}=44.7\pm0.4.$$

The uncertainties for $r_{\rm C}$, $r_{\rm Q}$, $\delta_{\rm C}$ and $\delta_{\rm Q}$ are much smaller than the combined fit. This is due to use of the full angular information.

2.6 Application to experimental data

When applied to experimental data, the angular distributions should be corrected for the detection efficiency, and the background events should be taken into account. Although the situations could be different in different experiments, we describe here how to deal with them in general.

The efficiency can be obtained by Monte Carlo simulation. For 0), 1), 2), 3) and 4) distributions of the experimental data, the count of each bin should be divided by the efficiency in that bin. In the full fit, we should include the efficiency function in the likelihood. The efficiency function can be obtained by fitting to the efficiency histogram with a suitable function.

For the background, we should identify all the sources. For each source, we obtain its angular distribution function. We then include the distribution functions of all sources into each fit function. In such a way, the contributions of the signal and each background component can be evaluated. The parameters of the signal will not be affected if we model the background correctly.

2.7 Electromagnetic form factors

$|G_{\rm C}|$, $|G_{\rm M}|$ and $|G_{\rm Q}|$ can be obtained from Equations (8), (9), (10), (25) and (26):

$$|G_{\rm M}|=\frac{1}{r}\sqrt{\frac{\sigma_0}{8\pi K(r_{\rm C}^2+\frac{4}{3}+8r_{\rm Q}^2)}}, \tag{72}$$

$$|G_{\rm C}|=rr_{\rm C}|G_{\rm M}|, \tag{73}$$

$$|G_{\rm Q}|=\frac{3}{r}r_{\rm Q}|G_{\rm M}|. \tag{74}$$

σ_0 above is the Born cross section. The Born cross section is obtained by making radiative corrections to the observed cross section. This accounts for initial state radiation. The initial state radiation also causes loss of the total energy, and variation of the form factors. This effect could be negligible, however, if we select events with the energy loss small enough.

Since we defined $\delta_{\rm M}=0$, the $\delta_{\rm C}$ and $\delta_{\rm Q}$ we obtained are actually $\delta_{\rm C}-\delta_{\rm M}$ and $\delta_{\rm Q}-\delta_{\rm M}$, respectively.

In this way, the magnitudes and relative phases of $G_{\rm C}$, $G_{\rm M}$ and $G_{\rm Q}$ can be determined. For uncertainties of the quantities, the covariance of the parameters should be taken into account.

3 Summary

We have described a method for measuring the charge, magnetic and quadrupole form factors of the D^* meson at time-like momentum transfer in e^+e^- annihilation. Table 1 lists an estimation of the number of $e^+e^-\to D^{*+}D^{*-}$ events in data samples of the BESIII and Belle experiments. The expectation for Belle II, which will 50 times as much data as Belle, is also given. The estimation uses the measured $e^+e^-\to D^{*+}D^{*-}$ cross sections [5, 6]. We suggest measuring the D^* electromagnetic form factors in e^+e^- experiments with this method. The method may also be applied to other vector particles such as ρ. The perturbative QCD prediction in Ref. [4] can be tested with experimental measurements. Measuring q^2 dependence of the electromagnetic form factors will provide useful information on hadron structure.

Table 1. Estimation of the number of $e^+e^-\to D^{*+}D^{*-}$ events in data samples of the BESIII, Belle and Belle II experiments. Belle II will have 50 times more data than Belle.

experiment	$\sqrt{s}$/GeV	luminosity /fb^{-1}	events
BESIII	4.18	3	9,200,000
BESIII	4.36	0.5	550,000
BESIII	4.416	1.1	1,100,000
Belle	10.58	711	390,000
Belle II	10.58	711 × 50	20,000,000

References

1 L. Durand, Phys. Rev., **123**: 1393 (1961)
2 H. Jones, Nuovo Cimento, **26**: 790 (1962)
3 R. Arnold, C. Carlson, and F. Gross, Phys. Rev. C, **21**: 1426 (1980)
4 S. Brodsky and J. Hiller, Phys. Rev. D, **46**: 2141 (1992)
5 G. Pakhlova et al (Belle Collaboration), Phys. Rev. Lett., **98**: 092001 (2007)
6 T. Uglov et al (Belle Collaboration), Phys. Rev. D, **70**: 071101 (2004)